Stability of elastic icosadeltahedral shells under uniform external pressure: Application to viruses under osmotic pressure

Antonio Šiber[1,*] and Rudolf Podgornik[2,3]
[1]*Institute of Physics, P.O. Box 304, 10001 Zagreb, Croatia*
[2]*Department of Theoretical Physics, Jožef Stefan Institute, SI-1000 Ljubljana, Slovenia*
[3]*Department of Physics, University of Ljubljana, SI-1000 Ljubljana, Slovenia*
(Received 25 May 2008; revised manuscript received 28 August 2008; published 26 January 2009)

We discuss the stability of icosadeltahedral shells subjected to a uniform external load in the form of an isotropic pressure. We demonstrate that there exists a universal critical buckling pressure scaling form that defines a locus of buckling instabilities. The parameter that uniquely determines this scaling form is shown to be the Föppl–von Karman number of nonpressurized shells. Numerical results are interpreted in terms of scaling forms for buckling instabilities of spheres and cylinders under isotropic mechanical pressure, and are applied to the case of viruses under osmotic pressure.

DOI: 10.1103/PhysRevE.79.011919 PACS number(s): 87.15.La, 46.70.−p, 46.32.+x

It has been experimentally demonstrated that microscopic and nanoscopic capsules can buckle and even collapse under external pressure, evaporation of solvent, or point forcing [1,2]. In most of these cases, the studied capsules were nearly spherical. Viruses represent an exception as they can take on more complicated shapes. Even icosahedral viruses that are studied in this article display a plethora of different shapes, some of them nearly perfectly spherical, while others have pronounced polyhedral shape and nearly flat faces [3]. These viruses can be represented as triangulated shapes of spherical topology with an icosa(delta)hedral backbone—this is known as the principle of quasiequivlence and forms the basis of the Caspar-Klug classification of icosahedral viruses [4]. This also means that viruses can be thought of as consisting of $10(T-1)$ clusters of hexamers and 12 clusters of pentamers, where T is the triangulation number of the virus [5,6].

The central issue of this work is to explore whether and how the equilibrium shape of an icosadeltahedral shell (viral capsid in particular) influences its response to the external isotropic pressure. This should be important for empty viral capsids submitted to osmotic pressure of the external solution. The impenetrability of the viral capsid to the osmoticant, such as polyethylene glycol (PEG), gives rise to a mechanical pressure across the capsid shell that compresses it. Experiments along these lines on complete virions are performed on bacteriophages in PEG bathing solutions [7].

By applying the continuum elasticity theory to viral capsids (empty viruses), Lidmar, Mirny, and Nelson [5] (LMN) have shown that their shape can be understood in terms of a *single* parameter, the so-called Föppl-von Kàrmàn (FvK) number (γ) given as

$$\gamma = Y\langle R\rangle^2/\kappa. \tag{1}$$

Here Y and κ are the two-dimensional Young's modulus and the bending rigidity of the viral protein sheet, respectively, and $\langle R\rangle$ is the mean radius of the viral capsid. For γ smaller than about 250, the equilibrium shape of the capsid that minimizes its elastic energy is practically a perfect sphere [see Fig. 1(b)]. When $250 \lesssim \gamma \lesssim 5000$, a continuous transition in equilibrium shape takes place and the capsids assume a more aspherical shape. LMN have termed this the "buckling transition" since the regions surrounding the pentagonal disclinations (protein pentamers) "buckle outward," away from the interior of the sphere so that the surface surrounding each of the disclinations is nearly conical (it should be understood that the buckling transition in the LMN terminology is not a consequence of any external forcing of the capsid, but simply results from the minimization of elastic energy of the shell [8]). In the region $250 \lesssim \gamma \lesssim 10^4$, the shape of the capsids can be represented as a union of 12 conical frusta with apices at the icosahedron vertices, which are fastened together at their bases [5,9]. This approximate representation of the exact shape provides a good account of the energetics of the shells [5,6]. In the range $10^4 \lesssim \gamma \lesssim 10^6$, the conical description of the shell becomes less satisfactory [cf. Fig. 6 of Ref. [5] and Fig. 1(b)] since another creeping transition takes place that flattens the icosahedron faces and sharpens the regions around their edges. This effect has been explained by Witten and Li [10] and Lobkovsky [11] as originating from the stretching energy along the edges, which becomes prohibitively large as the shell size increases (or as γ increases) and the curvature remains distributed along a large area of the shell. The scaling relations that are characteristic for the ridge sharpening are observed [5] when $\gamma \gtrsim 10^6$. The borders of different regimes of the FvK number are quite smeared, especially towards the ridge-sharpening regime, since the transitions in shell shapes are continuous [5].

Since the equilibrium shape of the capsid or shell changes with its FvK number, we could *a priori* expect that the response of the shells to external forcing in the form of an isotropic pressure is also strongly influenced by its FvK number. An intriguing question to pose in this context is whether the FvK number uniquely determines the elastic response of the shells to an external pressure. This has in fact been proven in Ref. [12] in as far as it concerns the dependence of the elastic susceptibility of shells, subjected to ex-

*asiber@ifs.hr

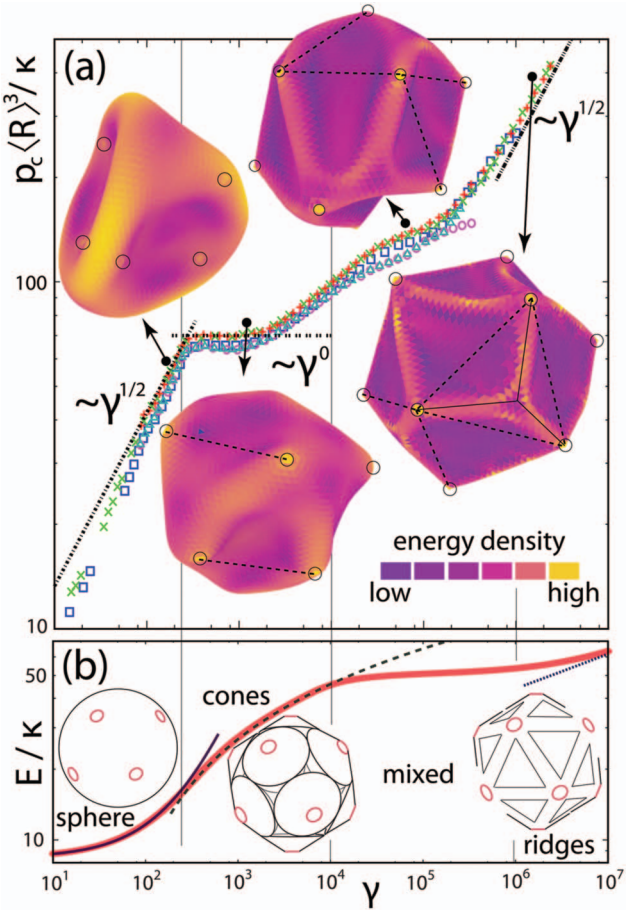

FIG. 1. (Color) (a) Scaled critical pressures (symbols) of the icosadeltahedral shells with $\epsilon=1$ and $T=441$ (+), $\epsilon=10$ and $T=441$ (×), $\epsilon=5$ and $T=100$ (squares), $\epsilon=5$ and $T=49$ (circles), and $\epsilon=4$ and $T=73$ (triangles) as a function of the FvK number γ. In these calculations, $u=0.005a$, ϵ was kept fixed, and κ was varied so as to produce a variation in γ. Thick dashed lines show scalings with γ as discussed in the text. The insets show the buckled shell shapes for different FvK numbers as denoted. (b) The energetics of nonpressurized shells as a function of γ. The regimes in which the shell can be represented as a sphere, an assembly of cones or ridges is indicated. Analytical expressions for the shell energetics are indicated by solid (sphere), dashed (cones), and dotted (ridges) lines [5]. Lines connecting neighboring disclinations in the nonpressurized state are indicated as dashed lines in the insets.

ternal forcing, on their FvK number. In contrast, moreover, we shall be interested in the (inward) buckling [8] of shells under pressure, which leads to a loss of icosahedral symmetry and a discontinuous change in the shell volume.

We model the shell as a polyhedron with icosahedral order whose neighboring vertices are connected with springs, so that the stretching energy is given by

$$H_s = \frac{\epsilon}{2}\sum_{i,j}(|\mathbf{r}_i - \mathbf{r}_j| - a)^2, \tag{2}$$

where ϵ is the spring constant, a is the equilibrium separation of the neighboring (i and j) vertices, and $\mathbf{r}_i$ is the vector pointing at the ith vertex. The bending energy of the shell is given by

$$H_b = \frac{\tilde{\kappa}}{2}\sum_{I,J}(\mathbf{n}_I - \mathbf{n}_J)^2, \tag{3}$$

where I and J are two polyhedron faces sharing an edge and $\mathbf{n}_I$ ($\mathbf{n}_J$) is the unit normal of the Ith (Jth) face. The macroscopic elasticity constants of the shell material can be derived from ϵ and κ as demonstrated in Ref. [5], so that the Young's modulus is $Y=2\epsilon/\sqrt{3}$, the (mean) bending rigidity $\kappa=\sqrt{3}\tilde{\kappa}/2$, the Gaussian bending rigidity $\kappa_G=-4\kappa/3$, and the Poisson ratio $\nu=1/3$. The shape of the shell under external pressure (p) is found by minimizing the total Hamiltonian of the problem,

$$H = H_s + H_b + pV, \tag{4}$$

where V is the shell volume. For a given shell T number and parameters a, ϵ, and κ, the nonpressurized shape of the shell is uniquely determined by its FvK number. Upon increasing the pressure, the shape that minimizes H in Eq. (4) changes; i.e., the shell deforms. We perturb the thus obtained shape by adding a random displacement to each of the vertices, $\mathbf{r}_i' = \mathbf{r}_i + u\mathbf{e}_i$, where $\mathbf{e}_i$ is a random three-dimensional unit vector, different for each vertex, and u is the amplitude of the displacement. The perturbed shape can be thought of as a particular conformation excited by (low-, $u \ll a$) temperature fluctuations. The perturbation has in general nonvanishing projections on each of the vibrational eigenmodes of the shell (see below). We then again minimize the energy of the perturbed shape. For pressures below a critical value, the shape equilibrates back to the unperturbed state with icosahedral symmetry. However, at some critical pressure (p_c), the new conformation that is adopted by the shell differs from the unperturbed state; i.e., a discontinuous transition in the shell shape parameters and volume is observed. We assume that this shape transition takes place prior to the complete rupture of the shell. This assumption is consistent with experiments on empty bacteriophage capsids, which are shown to withstand large forces and indentations by the tip of an atomic force microscope (~6 nm) prior to the onset of nonlinear response and possible rupture [13]. To relate our results with those on nonpressurized icosadeltahedral shells [5,6] and continuum theories of shell instability [15,16], we shall be particularly interested in shells with large T numbers. The results should be therefore directly applicable to viruses with large number of protein subunits, although the numerical simulations can be even more easily performed for shells with small T numbers.

Deformations of elastic shells subjected to external forces are known to belong to two distinct categories, depending on their elastic parameters. It has been experimentally demonstrated that deformations of a clamped half-cylindrical surface under point forcing [17] and the gravity-induced draping of naturally flat, isotropic sheets can be understood in terms of the creation of conical singularities (the so-called d cones) [18]. This means that the energy of deformation is dominantly of the *bending* type. On the other hand, the crumpling of a sheet of paper has been described as domi-

nated by the generation of narrow stretching ridges [19]. In this case, the energetics of deformation is steered by an interplay between bending and stretching contributions to elastic energy [11]. Both types of deformations can be seen in the shapes and energetics of equilibrium nonpressurized icosadeltahedral shells in different regimes of their FvK number [5]. Thus, we expect that the same two types of deformations should also be seen in the energetics of the shell buckling and this is one of the central issues of this work.

LMN have demonstrated [5] that the elastic energy of nonpressurized shells scales as $E \propto \kappa f(\gamma)$, where the function $f(\gamma)$ assumes different forms depending on the value of γ. A simple analysis suggests that if there is universality in the critical pressure and if it is related to the nonpressurized energetics and shape of the shell, it should reveal itself in the scaling $p_c' \rightarrow p_c \langle R \rangle^3 / \kappa$, where $\langle R \rangle$ is the mean radius of the nonpressurized shell. The results presented in Fig. 1(a) convincingly demonstrate the universality in p_c'. This figure displays the scaled critical pressures p_c' as a function of FvK number of the shell in the nonpressurized state. Note that the thus rescaled pressures for shells of different elastic properties (Y and κ) and T numbers (i.e., $\langle R \rangle$ if a is fixed) all fall on the same universal curve, which we denote by $\mathcal{U}(\gamma)$. The critical pressure thus assumes a scaling form

$$p_c = \frac{\kappa}{\langle R \rangle^3} \mathcal{U}(\gamma), \tag{5}$$

where $\mathcal{U}(\gamma)$ is a complicated scaling function.

What is the nature of the instability at $p = p_c$? Examination of the calculated shapes just above the critical pressure [see insets in Fig. 1(a)] shows that they display various types of inward buckling [8] (see below). The inward buckling of shells at the instability point p_c can be elucidated by analyzing their elastic eigenmodes as a function of pressure. These are obtained by diagonalizing the Hessian matrix of the Hamiltonian in Eq. (4)—viz., $\partial^2 H / \partial \mathbf{r}_i \partial \mathbf{r}_j$. At critical pressure there emerges an elastic soft mode, with zero eigenfrequency, that points to the existence of an instability of the shell with respect to the deformation in the direction of the eigenvectors of the soft mode. A similar type of soft-mode analysis has been successfully applied to the case of a ridge-buckling instability [20]. We find that the eigenvector configurations of the soft modes, describing different unstable elastic deformations, depend *crucially* and *solely* on γ, corroborating the scaling form, Eq. (5). Furthermore, the soft mode breaks the symmetry of the shell and steers its shape towards inward buckling.

Analytical approaches to (inward) shell buckling and collapse, even for perfectly spherical shells, are enormously complex and have occupied applied mathematicians and engineers for decades (see, e.g., Ref. [14]). This body of fundamental work enables us to gain valuable insight into our numerical results by providing analytical approximations to the scaling function $\mathcal{U}(\gamma)$ derived in the context of (inward) buckling of spheres [14–16] and cylinders [16] under external isotropic loads. Namely, although the shapes of both pressurized and unpressurized shells are fairly complex, their surface can be separated into regions that are locally isomorphous to spheres (two finite radii of curvature) or cylinders (one radius of curvature tending to infinity), depending on the FvK number. We thus expect that the scaling function $\mathcal{U}(\gamma)$ of the form that corresponds to buckling pressures of spheres and cylinders should be seen in our numerical data in different regimes of γ.

For FvK numbers smaller than about 250, the equilibrium shape of the unpressurized shell is practically a perfect sphere [5,6]. Therefore, the critical pressures should be proportional to

$$p_c^{\text{sphere}} \propto \frac{\kappa \sqrt{\gamma}}{\langle R \rangle^3}, \tag{6}$$

which is an expression for (inward) buckling pressure of thin spheres [15,16]. The $\sqrt{\gamma}$ scaling is exactly what we observe numerically in the region $90 \lesssim \gamma \lesssim 250$, as can be clearly seen from Fig. 1. A deviation from this scaling occurs for $\gamma < 90$. Note, however, that for a shell made of a uniform elastic material, $\gamma = 12(1-\nu^2)(R/d)^2$, where d is the effective thickness of the shell. Thus, for $\gamma \lesssim 90$, R/d is no longer negligible and an expression for thin shells in Eq. (6) becomes inapplicable. For shells that underwent the outward buckling [8] transition in their nonpressurized state, the shell surface is nearly conical around the pentagonal disclinations (protein pentamers)—i.e., it is locally cylindrical—so that the critical pressure should be proportional to [16]

$$p_c^{\text{cylinder}} \propto \frac{\kappa}{R_{cyl}^3}, \tag{7}$$

where R_{cyl} is the maximum radius of the cylindrical regions of the shell. This in its turn suggests that the deformation leading to inward buckling is concentrated at the midpoints of icosahedron faces. The maximum radii of the cones are $R_{cyl} \sim \langle R \rangle$, so that the critical pressures should be independent of γ—i.e., $\mathcal{U}(\gamma) \propto \text{const}$. This can be clearly discerned also from numerical results for $300 \lesssim \gamma \lesssim 3000$. As the FvK number increases further, the shell shape just prior to (inward) buckling shows flattening of the faces and concentration of curvatures along the icosahedral ridges, so that the radius of cylindrical regions immediately before (inward) buckling notably decreases from its nonpressurized value. This can be seen as an increase in the critical pressure—i.e. its deviation from the constant value predicted by Eq. (7). Note also that the description of shells in terms of cones becomes inaccurate when $10^4 \lesssim \gamma \lesssim 10^6$ [see Fig. 1(b)] and neither ridges nor cones provide an adequate description of the shell shape in this region of FvK numbers, since the curvature along ridges scales in a complicated way with R and γ. When $\gamma \gtrsim 10^6$, the ridge-sharpening transition gradually takes place and the characteristic curvature radii of (nonpressurized) ridges scale as [11] $R_{cyl} \propto \langle R \rangle \gamma^{-1/6}$, which means that the critical pressures should scale as

$$p_c^{\text{ridge}} \propto \frac{\kappa}{R_{cyl}^3} \propto \frac{\kappa \sqrt{\gamma}}{\langle R \rangle^3}, \tag{8}$$

which is functionally the same as for shells that are spherical in their nonpressurized state [$\gamma \lesssim 250$; see Eq. (6)], but for

different reasons. The scaling of p_c with $\sqrt{\gamma}$ in this regime is again strongly suggested by our numerical results.

A useful addition to this analysis can be obtained from a study of buckled shapes after the instability. However, in order to do this, one has to account for interactions between vertices that are not nearest neighbors since the buckling shell shows a tendency to self-intersect (this effect may even lead to formally negative volumes of the buckled shells). This means that topologically distant regions of the shell may become physically close in the buckled shape. We have approximately accounted for this effect by positioning a soft, exponentially repulsive potential in the geometrical center of the shell in its nonpressurized state. This potential acts on all vertices of the shell. We have checked that such a device does not change the critical pressures significantly and that various choices of the parameters of the potential (all of which produce nearly the same critical pressures as in the case of zero mean-field potential) do not influence the buckled shape in any important aspect. We have also found that the buckled shapes are compatible with the displacement patterns of the soft modes that lead to instability which gives additional credibility to our method.

The equilibrium shapes for pressures just above p_c—i.e., just after the (inward) buckling instability [see insets in Fig. 1(a)]—show a very complicated structure that we analyze only in broad outlines. For each particular γ the character of the buckled shape is directly related to the symmetry of the corresponding soft mode calculated before. For $\gamma<250$ buckled shells can be described as spheres with several inverted spherical caps [21] (three in the case of shape with $\gamma=190$). The icosahedral nature of the shell apparently does not interfere with the buckling event as can be seen from the total inversion of several pentagonal disclinations. This is not the case for the shape with $\gamma=1520$, whose disclinations remain prominent even in its buckled state, characterized by an inversion of regions surrounding the lines connecting two disclinations in the nonpressurized state (denoted by dashed lines in the insets) and corresponding to incipient icosahedral ridges for higher FvK numbers. A similar buckling scenario is even more evident for $\gamma=85\,000$. This shape can be described as a network of meandering ridges connecting pentagonal disclinations and bordering the large valleylike regions of inverted curvature. Note also that the ridges in the buckled state often meet in triplets at positions that are close to the centers of icosahedral faces in the nonpressurized state. Upon yet further increase, for $\gamma=1\,500\,000$, one observes that the ridges break up at the expense of prominent popping out of the icosahedron faces that they border. Alternatively, this mechanism can also be described as the repositioning of the ridges and creation of new ridge meeting points close to the centers of the icosahedral faces in the nonpressurized state.

Note also that the change in volume upon buckling progressively *decreases* as the FvK number increases. The nature of the reduction in volume can be particularly clearly discerned for shells with $\gamma\gtrsim 10^4$. In this case the ridges surrounding a face become unstable, break down, and invert, pushing the regions of large curvature towards other ridges that absorb it. Concurrently the ridges merge forming triplets at meeting points, usually at the center of the face that was bordered by the three collapsing ridges. In this way a large area of inverted curvature is formed that leads directly to a reduction in the shell volume.

We have shown that the salient features of our numerical results on the (inward) buckling of elastic icosadeltahedral shells under uniform external pressures can be understood on the basis of buckling instability pressures characteristic of surfaces with spherical and cylindrical topology. Since for viral capsids the estimated bending rigidity is $\kappa\sim 40k_BT$ [6] [a lower value of about $(10-15)k_BT$ has been found in Ref. [22]] and a typical radius is $\langle R\rangle\sim 30$ nm (for, e.g., λ-bacteriophage), one is led to critical pressures of about $p_c\sim 5$ atm in the regime of FvK numbers that are typical for large viruses ($\sim 10^3$). The pressures of this order of magnitude can be easily achieved in experiments with *empty* viral shells by applying the appropriate osmotic stress [7].

A.Š. acknowledges support by the Ministry of Science, Education and Sports of the Republic of Croatia through Research Project No. 035-0352828-2837. R.P. acknowledges support of the Agency for Research and Development of Slovenia (Grants No. P1-0055, No. Z1-7171, and No. L2-7080).

[1] A. Fery and R. Weinkamer, Polymer **48**, 7221 (2007).
[2] W. S. Klug, R. F. Bruinsma, J. P. Michel, C. M. Knobler, I. L. Ivanovska, C. F. Schmidt, and G. J. L. Wuite, Phys. Rev. Lett. **97**, 228101(2006).
[3] T. S. Baker, N. H. Olson, and S. D. Fuller, Microbiol. Mol. Biol. Rev. **63**, 862 (1999).
[4] D. L. D. Caspar and A. Klug, Cold Spring Harbor Symp. Quant. Biol. **27**, 1 (1962).
[5] J. Lidmar, L. Mirny, and D. R. Nelson, Phys. Rev. E **68**, 051910 (2003).
[6] A. Šiber, Phys. Rev. E **73**, 061915 (2006).
[7] A. Evilevitch *et al.*, Proc. Natl. Acad. Sci. U.S.A. **100**, 9292 (2003).
[8] We contrast outward buckling in the LMN case, thus without any external forcing, with inward buckling that we analyze here, in the presence of external isotropic pressure acting on the shell. We refer to the latter also simply as buckling, where the meaning is clear and there is no possibility of confusion.
[9] J. Tersoff, Phys. Rev. B **46**, 15546 (1992).
[10] T. A. Witten and H. Li, Europhys. Lett. **23**, 51 (1993).
[11] A. E. Lobkovsky, Phys. Rev. E **53**, 3750 (1996).
[12] M. Widom, J. Lidmar, and D. R. Nelson, Phys. Rev. E **76**, 031911 (2007).
[13] I. Ivanovska *et al.*, Proc. Natl. Acad. Sci. U.S.A. **104**, 9603 (2007).
[14] G. H. Knightly and D. Sather, Arch. Ration. Mech. Anal. **72**, 315 (1980).
[15] A. V. Pogorelov, *Bending of Surfaces and Stability of Shells*

(American Mathematical Society, Providence, RI, 1988).
[16] S. P. Timoshenko and J. M. Gere *Theory of Elastic Stability* (McGraw-Hill, New York, 1985).
[17] A. Boudaoud *et al.*, Nature (London) **407**, 718 (2000).
[18] E. Cerda *et al.*, Nature (London) **401**, 46 (1999). E. Cerda, L. Mahadevan, and J. M. Pasini, Proc. Natl. Acad. Sci. U.S.A. **101**, 1806 (2003).
[19] E. M. Kramer and T. A. Witten, Phys. Rev. Lett. **78**, 1303 (1997); T. A. Witten, Rev. Mod. Phys. **79**, 643 (2007).
[20] B. A. DiDonna, Phys. Rev. E **66**, 016601 (2002).
[21] C. Quilliet, Phys. Rev. E **74**, 046608 (2006).
[22] T. T. Nguyen, R. F. Bruinsma, and W. M. Gelbart, Phys. Rev. E **72**, 051923 (2005).